Journal of Thermal Analysis and Calorimetry, Vol. 90 (2007) 3, 777–782

ZINC COATINGS FOR OXIDATION PROTECTION OF FERROUS SUBSTRATES
Part II. Microscopic and oxidation mechanism examination

G. Vourlias, N. Pistofidis, E. Pavlidou and K. Chrissafis[*]

Physics Department, Aristotle University of Thessaloniki, Thessaloniki 54124, Greece

A common phenomenon in the process industries is the oxidation of the exterior surface of steel pipes used in superheated steam or hot oils networks. For their protection different coatings could be used. In the present work the performance of zinc coatings deposited with hot-dip galvanizing, pack cementation and thermal spraying was considered, in order to protect industrial equipment up to 400°C. For that purpose coated carbon steel coupons were exposed at 400°C and their behavior was examined with light microscopy, scanning electron microscopy and X-ray diffraction.

Thermogravimetric analysis was also used in order to observe in situ the oxidation phenomena. From this investigation it was deduced that in every coating a scale is formed that is mainly composed of ZnO, while Fe oxides were also detected in galvanized and pack coatings. The growth of this scale took place at the metal/scale interface. Moreover, as far as it regards the kinetics of the oxidation, it was concluded that the increase of the mass of the specimens is a function of the square root of the exposure time, which means that the scale formed is rather protective for the underlying zinc. From the above observation it seems that the behavior of zinc coatings would be excellent at 400°C. However, the presence of the Fe/Zn phases inside the galvanized and pack coatings led to the formation of cracks, which could expose the substrate and thus destabilize the coating. This phenomenon does not take place in the thermal sprayed coatings, where the Fe/Zn phases are absent.

Keywords: *coating materials, oxidation, scanning electron microscopy, thermal analysis, X-ray diffraction, zinc*

Introduction

An important problem encountered in the process industries is the corrosion and oxidation of the outer surface of steel pipes used for the transportation of superheated steam and hot oils [1]. This phenomenon is due to the reaction of steel with the atmospheric oxygen, which causes oxidation when the system is hot, and to the effect of moisture that condensates between the pipes and their insulation, when the system cools down. In order to inhibit these phenomena and to protect the piping installations, organic or inorganic coatings are often used [1]. A common material for applications of this kind is zinc silicate, which is resistant up to 400°C [1]. However, the protective action of this coating is limited as far as it concerns moisture, which could cause its destabilisation. A more effective solution is the application of stainless steel tubes, which, although they are very efficient and resist both oxidation and corrosion, are very expensive [2].

An alternative method that could be used instead, is the application of metallic zinc coatings [3]. The usage of these coatings is compatible with the end-use of the coated pipes, because they could be applied only at the outer surface, as in the case of organic or other inorganic coatings. Furthermore, extended and very accurate researches indicate that they are very resistant to wet (aqueous) corrosion [4–17], as in the case that was previously mentioned.

Their performance at 400°C was roughly estimated in a previous work of ours [18]. In this work the macroscopic behaviour of different zinc coatings (hot-dip galvanized, thermal sprayed and pack coatings) was examined. From this research it was deduced that every zinc coating, which was examined, is covered by a scale mainly composed by ZnO. Iron oxides were also detected in the case of the galvanized and pack coatings. Both these oxides are expected to inhibit the zinc oxidation and consequently to protect the ferrous substrate. However, in the case of galvanized and pack coatings a crack network was formed on their surface due to the mismatch of the thermal expansion coefficients of the coating and the substrate. This network offers paths to the oxygen ions. Thus, it seems that it facilitates oxidation. Nevertheless, the zinc protection even in the case of cracks is not inhibited, because zinc is anodic to steel [4].

As a result, the macroscopic examination implies that zinc coatings are effective for oxidation protection up to 400°C. Nevertheless, in order to have more accurate long-term predictions, the oxidation mechanism has to be clarified. For this purpose in this work

* Author for correspondence: hrisafis@physics.auth.gr

1388–6150/$20.00

Akadémiai Kiadó, Budapest, Hungary
Springer, Dordrecht, The Netherlands

microscopic methods associated with thermal analysis are used in order to study oxidation. This way the verification of the macroscopic conclusions would be possible. For comparison reasons a coupon of bare steel was exposed in the same conditions and examined with the same methods. This action allowed a more precise estimation of the effectiveness of zinc.

Experimental

Materials used – coating methods

Commercial, hot-rolled low carbon steel sheets were used as substrates for the sample preparation. The same steel was used for the preparation of the bare coupon exposed in the same conditions. The steel designation was U St-34 (C≤0.17, Mn: 0.20–0.50, S≤0.05, P≤0.08). Rectangular coupons have been cut from the steel sheet with sizes ranging from 100 mm long×30 mm wide×3 mm thick to 5 mm long×3 mm wide×2 mm thick. The different sizes were necessary due to the different methods used for corrosion and characterization.

Hot-dip galvanizing took place in a Thermolyne 1400 electric furnace inside a graphite crucible. The dipping time was 3 min and the zinc temperature was 450±2°C. Prior to galvanizing, the coupons were degreased in a solution of a non-ionic tenside containing H_3PO_4, pickled (deoxidized) in an aqueous solution containing 16% HCl and fluxed in an aqueous solution containing 50% $ZnCl_2{\cdot}2NH_4Cl$. The average coating thickness of the hot-dip galvanized coatings, as it was determined metallographically, was about 80–100 μm.

Pack cementation was accomplished in porcelain crucibles, filled with powder mixture containing 2% NH_4Cl, 50% Zn and the rest Al_2O_3. The ferrous substrates were immersed in this mixture. The crucibles were sealed and placed in a tubular argon-purged electric furnace at 400°C for 60 min [11]. The average coating thickness for this method was close to the thickness of the hot-dip galvanized coatings (about 60–90 μm).

For the samples deposited with thermal spraying, a METCO 14E wire flame spray device was used. The distance between the flame and the substrate was 120 mm, the combustible gas was acetylene and the wire used had a 2.4 mm diameter and it was composed by 99.9% pure Zn. Prior to the coating deposition, the surface of the ferrous substrates was sandblasted. The thickness of the as-cast coatings was about 150–200 μm. The excessive thickness with regard to the methods mentioned before, is an inherent characteristic of thermal spraying.

Corrosion study – characterization methods

For the examination of the oxidation, the specimens were exposed in a laboratory electric furnace equipped with a ventilation system. The ventilation system ensured good air circulation, without affecting the atmospheric pressure in the furnace. The temperature of the furnace was settled at 400°C and the exposure time was 24 h. Samples of bare (uncoated) steel were also placed in the furnace for comparison reasons.

For the in-situ study of the oxidation of the coatings thermogravimetric measurements were used. They were carried out with a Setaram SETSYS TG-DTA 1750°C. The samples were placed in alumina crucibles. An empty alumina crucible was used as reference. For the isothermal experiments, the samples, at first, were heated from ambient temperature to 400°C in a 50 mL min^{-1} flow of air, with heating rate of 10°C min^{-1}. The samples remained for 24 h at this temperature. For comparison reasons a coupon of bare steel was also examined under the same conditions.

Apart from the TG, the usage of the laboratory furnace was considered necessary, because its size allows the examination of larger samples. In the present work, this fact has the advantage that the larger size of the samples offers more representative results, because it is closer to the scale of the objects used in real applications. On the other hand, TG offers the possibility to observe oxidation in situ, which is not possible with the laboratory furnace.

For the study of the corrosion, the surface of the oxidized coatings was initially examined with scanning electron microscopy with a 20 kV JEOL 840A SEM, equipped with an Oxford ISIS 300 EDS analyzer and the necessary software for point microanalysis, linear microanalysis and chemical mapping of the surface under examination. The coated surface of the samples was observed without any preparation.

Afterwards cross sections were cut from each sample, mounted in bakelite and polished down to 5 μm alumina emulsion. The as-prepared coupons were initially observed with an Olympus BX60 light microscope connected to a digital camera CCD JVC TK-C1381. The same samples after the same preparation procedure were also examined with the above mentioned SEM.

SEM was also used for the examination of the bare steel coupon. Furthermore a Karl Zeiss M8 low magnification binocular light microscope equipped with a CCD camera for image capture was also used, while the composition of the scale formed was determined with a 2-cycle SEIFERT 3003 TT diffractometer (CuK_α radiation) with Bragg–Brentano geometry.

Results and discussion

In previous works of ours [18, 19] zinc coatings were examined at 400°C, which is also the most suitable for industrial applications [1]. Consequently, a temperature of 400°C was chosen in the present work for all the isothermal experiments. The exposure of the specimens at this temperature resulted to the formation of a scale visible with naked eye which is mainly composed by ZnO. Fe oxides are also present in the case of hot-dip galvanized and pack coatings [18].

To identify the scale morphology along with its chemical composition, the surface of the coatings was examined with SEM associated with an EDS analyser (Figs 1–3).

An extended crack network is observed in the case of galvanized and pack coatings (Figs 1c, d and 2a). These cracks were observed also when the coating was examined at low magnification and their formation was interpreted based on the mismatch of the expansion coefficients of the coating and the substrate [18].

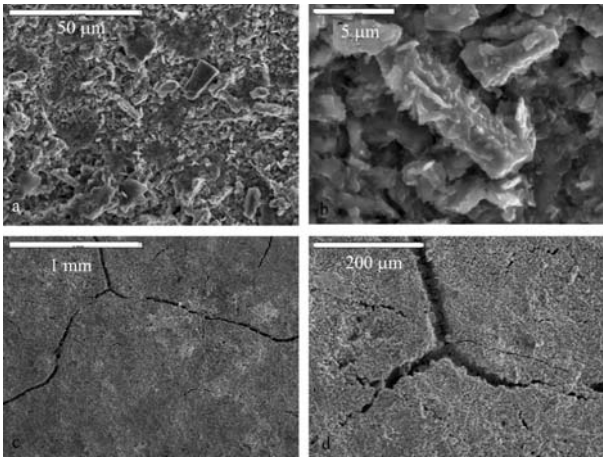

Fig. 1 SEM micrographs of the surface of a hot-dip galvanized coating after 24 h of exposure at 400°C; a and b – refer to different magnification of the same area, c and d – show a crack at different magnification

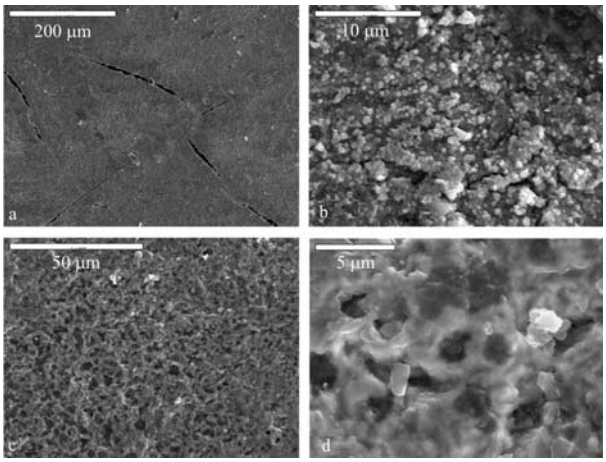

Fig. 2 SEM micrographs of the surface of zinc pack coating after 24 h of exposure at 400°C; a – shows a coating crack, b – refers to the microcrystalline area, c and d – show the porous film at different magnification

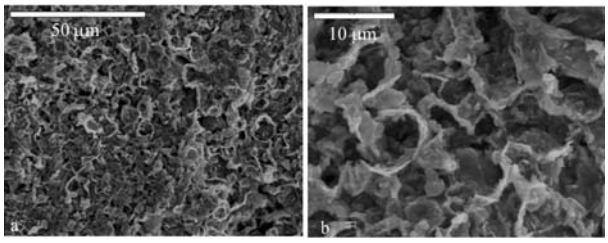

Fig. 3 SEM micrographs of the surface of thermal sprayed coating after 24 h of exposure at 400°C; a and b – refer at different magnification

Furthermore, crystals of different sizes and shapes are observed on the surface of every coating. In the case of galvanized coatings, they are long, almost rectangular (Fig. 1b) and they are composed by zinc and oxygen, hence by ZnO. Iron was also detected and locally, in some points, its content was up to 50 mass%.

Concerning pack coatings, two different areas were observed based on their relief. The majority of the coating surface seems to be covered by a rather rough film (Fig. 2c), while a microcrystalline phase is present at lower extent (Fig. 2b). Both these phases are composed mainly of ZnO, while Fe is also detected up to 10%. In the microcrystalline areas however, the iron content is much higher, up to 50%. Consequently, the different morphology could be attributed to the different iron content of the oxides formed, which is probably due to the rather non-uniform iron distribution in the non-corroded coating [13].

The micrographs of thermal sprayed coatings are more uniform (Fig. 3). There are no cracks, while a scale of uniform appearance is formed, which is composed only of ZnO. Iron oxides were not detected.

The above examination verified the conclusions about the composition of the scale on the oxidized samples as it was determined with XRD [18]. So, in the case of galvanized and pack coatings, the scale is composed by ZnO along with mixed Zn and Fe oxides. The composition of the thermal sprayed coatings is a little different because ZnO is only present, while Fe oxides or mixed Zn–Fe oxides are not detected, because the coating does not contain any iron.

Apart from the surface examination, the oxidized samples were also cut lengthwise and their cross-section was microscopically examined (Fig. 4). From these micrographs the thickness of the scale was measured, which after 24 h of exposure was similar in every coating and less than 10 μm in average.

These micrographs offer important information about the oxidation mechanism. What is rather impressive in every coating is the formation of a signifi-

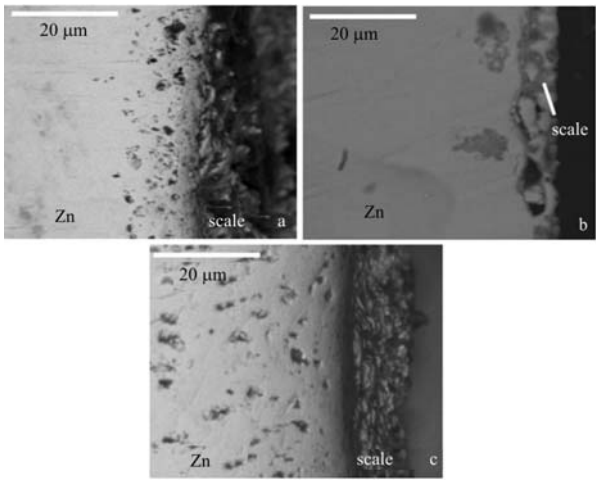

Fig. 4 SEM micrographs of the cross-section of a – a hot-dip galvanized, b – a pack and c – a thermal sprayed coating after 24 h of exposure at 400°C

cant volume of voids from both sides of the scale/coating interface. This phenomenon could be explained if we take into account that the growth mechanism of the coating is highly affected by the diffusivities of zinc and oxygen through the scale. As it is stated elsewhere [2, 20, 21], zinc diffusivity is many orders of magnitude higher than oxygen diffusivity. Consequently, for the combination of metal cations and oxygen anions and the scale formation, the migration of the cations takes place much faster. Thus the diffusion control results in the growth of the scale at the scale-gas interface, which is very usual for the common base metals (Fe, Ni, Cu, Cr, etc. [22]). When this growth mechanism is predominant, the high rate of cation outward diffusion results in the condensation of cation vacancies from both sides of the metal/scale interface, which finally form voids similar to those observed in Figs 4a–c.

The fact that the scale grows outwards is very beneficial for the effectiveness of the coatings under examination. When the scale growth takes place at the metal-scale interface, usually a large increase in volume is observed which introduces severe tensile stresses into the scale [22]. As a result fracture of the scale occurs. Furthermore, as the oxidizing species segregates to the scale/metal interface, it weakens this interface, which plays a critical role in blocking further corrosion. Finally, protection is not achieved. By contrast, growth at the scale/gas interface does not affect the stability of the scale, which is the case for ZnO.

In any case, the degradation of the examined coatings seems to be uniform. The metal/oxide interface is rather even (following the substrate roughness) while no preferential oxygen paths or preferentially oxidized grain boundaries into the bulk coating were observed. In a similar way, the results of the EDS analysis along straight lines of the cross-section of the

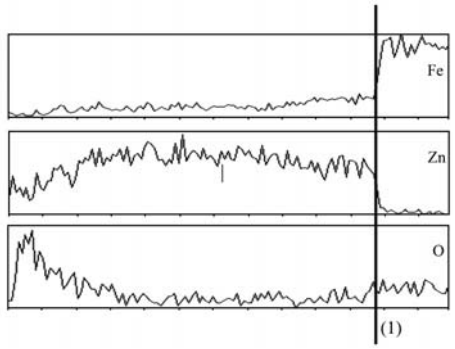

Fig. 5 Representative stoichiometric analysis with EDS along a straight line of the cross-section of a hot-dip galvanized coating after 24 h of exposure at 400°C; line 1 – refers to the coating/ferrous substrate interface

coupons, starting from the outer surface of the coating and finishing beneath the coating/substrate interface (Fig. 5), imply homogeneous oxygen diffusion into the coating. Hence the oxidation of the coating is uniform, while neither intergranular nor internal oxidation is observed. In general, these mechanisms are more probable when segregation of different phases at the grain boundaries is observed [5]. In the case of the coatings under examination, this phenomenon is not reported [4, 11, 19, 23]. This conclusion is very beneficial for the coating performance, because intergranular corrosion could lead to a fast destabilization and decomposition of the coating, since grains are detached from it, as their boundaries are preferentially corroded without the oxidation of the main part of each crystallite.

The above analysis offers many qualitative data on the oxidation mechanism. However for a better estimation of the coating performance TG was used which could also offer a quantitative estimation.

The thermogravimetric plot of the mass change per unit of surface for the different coatings *vs*. time after about 24 h of exposure at 400°C is presented in Fig. 6. However this plot is more useful if the square

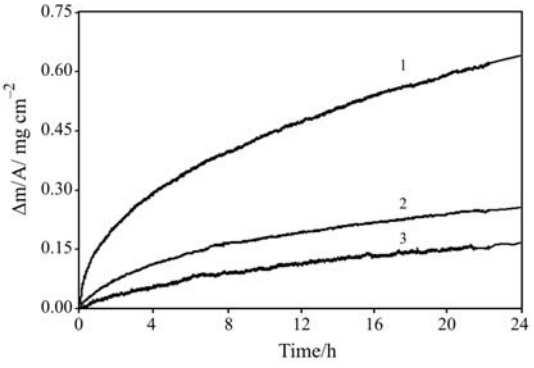

Fig. 6 Thermogravimetric plot of the mass change per unit of surface for the different coatings *vs*. time after about 24 h of exposure at 400°C; 1 – thermal spray coating, 2 – galvanized coating, 3 – pack cementation coating

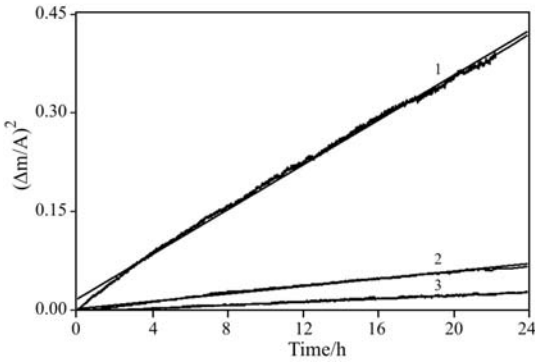

Fig. 7 Plot of the square mass change per unit of surface for the different coatings *vs*. time after 24 h of exposure at 400°C. The straight lines correspond to the trend lines of each curve and were drawn following the least squares; 1 – thermal spray coating, 2 – galvanized coating, 3 – pack cementation coating

of the mass change per surface unit as a function of time is plotted. In this case for every sample a straight line is drawn (Fig. 7). The deviations from the linear behavior, which are observed during the initial time values, are partially due to temperature variations until the target-temperature is obtained. This is an inherent limitation of the equipment used. In any case, the linear behavior indicates that the oxidation kinetics follows a parabolic equation of the type:

$$\left(\frac{\Delta m}{A}\right)^2 = k_p t \qquad (1)$$

where Δm refers to the mass change of the sample, A is the exposed surface, t is the exposure time and k_p is the rate constant. In the present work absolute values for k_p (and consequently absolute oxidation rates) were not determined, due to the uncertainty of the surface measurements, as it was previously explained.

However, the above equation would be very helpful for qualitative predictions on the oxidation resistance of each coating. This parabolic rate law assumes that the diffusion of metal cations or oxygen anions is the rate controlling step and it could be derived from Fick's first law of diffusion, if we assume that the mass change of the coating is proportional to the ionic flux, the concentrations of diffusing species at the metal-scale and gas-scale interfaces are constant and the diffusivities through the scale are invariant [22]. The last two assumptions imply that the oxide layer is uniform, continuous and composed by one single phase. These conditions are satisfied by ZnO, where the cation diffusion is predominant. In any case, the parabolic rate low is another factor that verifies good oxidation resistance, since the increase of the coating thickness reduces the oxidation rate, as the increased thickness delays the diffusion of the ions through the scale. Hence zinc coatings are expected to be resistant to oxidation also for longer exposure periods. Solid conclusions on this topic could be deduced only if long term experiments take place. Also, the effect of heating/cooling cycles is necessary to be assessed. However, the preliminary data gathered from this work are very encouraging and justify the continuance of this research.

A comparison of the above conclusions with those that concern bare steel is also beneficial for zinc. A scale is formed as well on the surface of bare steel under the same oxidation conditions. This phenomenon is clearly identified with naked eye (Fig. 8a). The analysis of the scale XRD pattern shows that it is composed by several different Fe oxides (Fig. 8b) (PDF#85-0987, PDF#89-0950, PDF#86-1337, PDF#89-0690 [24]) while the SEM observation of its cross-section (Figs 9a and b) indicates that its thickness is about 10 μm. However, the observed scale is not continuous. By contrast, it is interrupted by large gaps, which are also clearly distinguished in the form of cracks when its plain view is observed (Fig. 9c). This crack network is much denser than the network of the galvanized and pack coatings. Hence the iron degradation is expected to be faster. Nevertheless, if we take into account the fact that iron does not offer any protection when wet (aqueous) corrosion arises as in the case of insulated pipes, it is obvious that zinc coatings are more effective. As a result their usage for the oxidation protection of steam networks would be very beneficial, because apart from the fact that they offer efficient protection, their application is very easy and fast, which is an important advantage in the case of networks with the length of the steam networks.

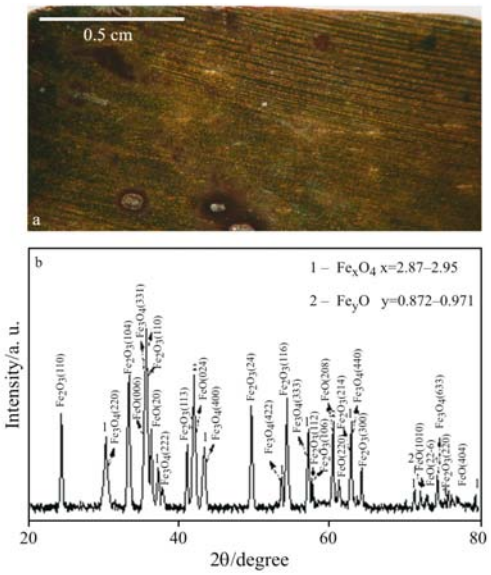

Fig. 8 a – Plain view photograph of the surface of bare steel sample after 24 h of exposure a – at 400°C and b – XRD pattern

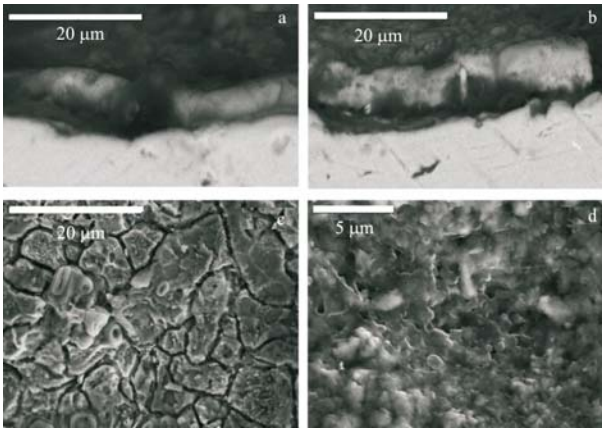

Fig. 9 SEM micrographs of a and b – the cross-section, c and d – the plain view of oxidized iron samples after 24 h of exposure at 400°C

Conclusions

Every zinc coating that was examined during the present work (galvanized, pack, thermal sprayed), when exposed in the air at 400°C is covered by a scale, which is primarily composed by ZnO. Iron oxides were also detected in the case of the galvanized and pack coatings. This scale grows in every coating at the metal/scale interface through cation (Zn^{2+}) diffusion through uniform oxidation. Neither intergranular nor internal corrosion were observed. Furthermore the scale growth, as described by the square mass change per surface unit *vs*. time, follows a parabolic law.

The above conclusions imply that the behavior of galvanized, pack and thermal sprayed zinc coatings would be excellent during heating for 24 h at 400°C. However, the presence of the Fe/Zn phases inside the galvanized and pack coatings leads to the formation of cracks in these coatings at 400°C. This phenomenon is not observed in the thermal sprayed coatings, where the Fe/Zn phases are absent. However, the zinc protection even in the case of cracks is not inhibited, because zinc is anodic to steel [4]. Hence every zinc coating (from the examined ones) could be used at 400°C, also for higher exposure periods. If we also take into account the fact that the growth of the zinc coatings is easy and inexpensive, it is obvious that they are characterized by a large number of advantages.

References

1 M. J. Mitchell, Developments in Coatings for High Temperature Corrosion Protection, Proceedings of the Society of Protective Coatings 2002 Technical Presentations, Tampa, Florida, November 3–6, 2002, pp. 88–96.
2 J. R. Davis, Ed., Heat-Resistant Materials, ASM International, New York 1997.
3 Zinc coatings, American Galvanizing Association, Englewood, Colorado 2000.
4 A. R. Marder, Prog. Mater. Sci., 45 (2000) 191.
5 X. G. Zhang, Corrosion and Electrochemistry of Zinc, Plenum Press, New York 1996.
6 S. Oesch and M. Faller, Corros. Sci., 39 (1997) 1505.
7 V. Ligier, M. Wery, J. Y. Hihn, J. Faucheu and M. Tachez, Corros. Sci., 41 (1999) 1139.
8 A. R. Mendoza and F. Corvo, Corros. Sci., 42 (2000) 1123.
9 E. Almeida, M. Morcillo and B. Rosales, Br. Corros. J., 35 (2000) 284.
10 E. Almeida, M. Morcillo and B. Rosales, Br. Corros. J., 35 (2000) 289.
11 G. Vourlias, N. Pistofidis, D. Chaliampalias, E. Pavlidou, P. Patsalas, G. Stergioudis, D. Tsipas and E. K. Polychroniadis, Surf. Coat. Technol., 200 (2006) 6594.
12 N. Pistofidis, G. Vourlias, E. Pavlidou, K. Chrissafis, G. Stergioudis, E. K. Polychroniadis and D. Tsipas, J. Therm. Anal. Cal., 84 (2006) 417.
13 N. Pistofidis, G. Vourlias, D. Chaliampalias, E. Pavlidou, K. Chrissafis, G. Stergioudis, E. K. Polychroniadis and D. Tsipas, J. Therm. Anal. Cal., 84 (2006) 191.
14 G. Vourlias, N. Pistofidis, G. Stergioudis and D. Tsipas, Cryst. Res. Technol., 39 (2004) 23.
15 G. Vourlias, N. Pistofidis, G. Stergioudis, E. Pavlidou and D. Tsipas, Phys. Stat. Sol. A: Appl. Res., 201 (2004) 1518.
16 N. Pistofidis, G. Vourlias, D. Chaliampalias, E. Pavlidou, G. Stergioudis and E. K. Polychroniadis, Surf. Interface Anal., 38 (2006) 252.
17 G. Vourlias, N. Pistofidis, D. Chaliampalias, E. Pavlidou, G. Stergioudis, D. Tsipas and E. K. Polychroniadis, Corros. Eng. Sci. Technol., 41 (2007) in press, (DOI: 10.1179/174327807x159899)..
18 G. Vourlias, N. Pistofidis, K. Chrissafis, El. Pavlidou and G. Stergioudis, J. Therm. Anal. Cal., (2007), accepted.
19 G. Vourlias, N. Pistofidis, D. Chaliambalias, K. Chrissafis, El. Pavlidou and G. Stergioudis, J. Therm. Anal. Cal., 87 (2007) 401.
20 G. W. Tomlins, J. L. Routbort and T. O. Mason, J. Appl. Phys., 87 (2000) 117.
21 P. Erhart and K. Albe, Phys. Rev. B, 73 (2006) 115207-1.
22 M. G. Fontana, Corrosion Engineering, 3rd Ed., McGraw-Hill, New York 1986.
23 R. H. Unger, ASM Handbook, Vol. 5 – Surface Engineering, New York, ASM International, 2000.
24 PC Powder Diffraction Files, JCPDS-ICDD, 2000.

Received: December 18, 2006
Accepted: January 25, 2007
OnlineFirst: March 23, 2007

DOI: 10.1007/s10973-006-8305-8